

Equation of state and spin-correlation functions of ultrasmall classical Heisenberg magnets

Orion Ciftja and Marshall Luban

Ames Laboratory and Department of Physics and Astronomy, Iowa State University, Ames, Iowa 50011

Mark Auslender

Department of Electrical and Computer Engineering, Ben-Gurion University, Beer-Sheva 84105, Israel

James H. Luscombe

Department of Physics, Naval Postgraduate School, Monterey, California 93943

(Received 26 March 1999; revised manuscript received 21 June 1999)

We obtain analytical expressions for the total magnetic moment and the static spin-correlation functions of the classical Heisenberg model for ultrasmall systems of spins (unit vectors), that interact via isotropic, nearest-neighbor (n-n) exchange and that are subject to a uniform dc magnetic field of arbitrary strength. Explicit results are presented for the dimer, equilateral triangle, square, and regular tetrahedron arrays of spins. These systems provide a useful theoretical framework for calculating the magnetic properties of several recently synthesized molecular magnets. The tetrahedron as well as the equilateral triangle systems, each considered for n-n antiferromagnetic exchange, are of particular interest since they exhibit frustrated spin ordering for sufficiently low temperatures and weak magnetic fields. [S0163-1829(99)01538-6]

I. INTRODUCTION

In recent years there has been a surge of interest in the magnetic properties of synthesized molecular clusters^{1,2} containing relatively small numbers of paramagnetic ions. With the ability to control the placement of magnetic moments of diverse species within stable molecular structures, one can test basic theories of magnetism and explore the design of novel systems that offer the prospect of useful applications.^{3,4} A common feature of these organic-based molecular magnets is that intermolecular magnetic interactions are extremely weak compared to those within individual molecules, i.e., a bulk sample can be described in terms of independent individual molecular magnets. As examples of molecular magnets with ultrasmall numbers of embedded paramagnetic ions we mention: Two dimer systems, one⁵ of V^{4+} (spin $S=1/2$) and the second consisting of $6 Fe^{3+}$ ions (spin $S=5/2$); a nearly equilateral triangular array⁷ of V^{4+} ; a nearly square array⁸ of Nd^{3+} (total spin $j=9/2$); a regular tetrahedron array⁹ of Cr^{3+} (spin $S=3/2$); and a nonregular tetrahedron array¹⁰ of Fe^{3+} ions. Also noteworthy is the pyrochlore antiferromagnet $Tb_2Ti_2O_7$, although distinct from the class of organic molecules yet sharing the feature that the Tb^{3+} ions (total spin $j=6$) reside on a network of very weakly coupled tetrahedra.¹¹

This paper has been motivated by the rapid experimental developments in the synthesis of molecular magnets with ultrasmall numbers of strongly interacting moments. It is perhaps surprising that for high-spin moments the calculation of equilibrium magnetic properties for arbitrary temperatures and magnetic-field strengths presents a serious challenge. One might expect that the determination of the partition function for a few-spin system would be a relatively simple task. To put this matter in perspective, it should be recalled that for a finite open chain of *classical* spins that interact

with nearest-neighbor (n-n) isotropic Heisenberg exchange, the partition function has been evaluated only in the absence of an external magnetic field.¹² For the related system, where the linear chain is closed so as to form a ‘‘Heisenberg ring,’’ the calculation of the partition function and the equilibrium equal-time spin-correlation function is extremely involved. Exact, unwieldy infinite series expansions of these quantities were successfully derived¹³ many years ago, but only for zero applied field. With the introduction of an external magnetic field the analytic calculation of the partition function has been an intractable problem even for small numbers of interacting moments.¹⁴

The purpose of this paper is to provide the full magnetic equation of state (molecular magnetic moment) and equal-time spin-correlation functions, versus temperature and applied magnetic field, for molecular magnets containing very small numbers of interacting classical moments. In more experimental terms, we calculate quantities that are directly related to the temperature and applied field-dependent magnetization. The assumed interaction between moments is n-n isotropic Heisenberg exchange. In particular, we treat the case of a dimer, and arrays of moments with the geometries of an equilateral triangle, a square, and a regular tetrahedron, to mirror some of the synthetic molecular magnets cited above. The special cases of the equilateral triangle and a regular tetrahedron of spins that interact via n-n antiferromagnetic exchange are of special interest because these systems^{7,11} exhibit frustrated order at sufficiently low temperatures and weak magnetic fields. Finally, we remark that the present results are needed as part of the analytical calculations¹⁵ of the *time-dependent* spin-correlation functions for these classical Heisenberg spin systems. The time-dependent spin-correlation functions are vital for deriving the analytical formulas for NMR and neutron-scattering measurements.

In Sec. II B, after summarizing several basic, general for-

mulas for a ring of N equally spaced spins described by the classical n-n Heisenberg model, we illustrate our method for evaluating the partition function for the case of $N=3$ spins (equilateral triangle) in the presence of an external magnetic field. In our calculations we exploit the fact that the Hamiltonian of the system is expressible solely in terms of the total spin vector, and this quantity is included in an extended phase-space integration. It is instructive to compare the classical Heisenberg results with the analogous quantum system with individual spins S , and this is also provided in Sec. II B. For the sake of completeness, we also list our major results for the regular tetrahedron in Sec II C and for the dimer in Sec II D. In Sec. III we focus on the rather complex case of a square array of spins with n-n interaction in the presence of the magnetic field. For this system, we derive the partition function after introducing a convenient pair of auxiliary variables to supplement the total spin vector and after integrating over a further extended phase space. For comparison purposes, we also provide results for the square array of quantum spins, with $S=1/2, \dots, 5/2$. Finally, in Sec. IV we summarize the present results and comment briefly on the obstacles to extending the present calculations to larger arrays of spins, e.g., rings of $N \geq 5$ spins with n-n interactions, while noting several larger systems that can be dealt with successfully.

II. CALCULATIONAL METHOD

A. General formulas

In this subsection we define our notation and list several standard thermodynamic relations for the classical Heisenberg model of a ring of N equally spaced spins. We suppose that the spins are coupled by n-n, isotropic exchange interactions and they also interact with a uniform dc external magnetic field \vec{B} . We write the Hamiltonian of the system as

$$H_N(B, J) = J \sum_{i=1}^N \vec{S}_i \cdot \vec{S}_{i+1} - \mu \vec{B} \cdot \sum_{i=1}^N \vec{S}_i. \quad (1)$$

The direction of \vec{B} defines the z (polar) axis, the spins \vec{S}_i are classical unit vectors whose orientations are specified by the polar and azimuthal angles, θ_i and φ_i , and these extend from 0 to π and 0 to 2π , respectively, and the cyclic boundary condition, $\vec{S}_{N+1} \equiv \vec{S}_1$, is applied. The n-n interaction between spins can be either antiferromagnetic (AFM), $J > 0$, or ferromagnetic (FM), $J = -|J| < 0$. The Hamiltonian of Eq. (1) provides the classical counterpart to the quantum Heisenberg model,

$$\hat{H}_N(B, J) = J_S \sum_{i=1}^N \hat{S}_i \cdot \hat{S}_{i+1} - g \mu_B \vec{B} \cdot \sum_{i=1}^N \hat{S}_i, \quad (2)$$

of atomic ion spins S (expressed in units of \hbar) with n-n exchange interaction J_S . (Here and later in the text the caret symbol will be used for quantum operators.) This correspondence is achieved by rescaling all quantum spin operators by the factor $\sqrt{S(S+1)}$. It thus follows that $J = S(S+1)J_S$ and the quantity μ in Eq. (1) is given by $\mu = (g \mu_B) \sqrt{S(S+1)}$, where g is the Landé g factor for the given ion and μ_B is the Bohr magneton. In subsequent sections of this paper we

compare results for the equilibrium magnetization and the n-n spin-correlation function for increasing values of S . The results rapidly approach the classical limit for increasing S .

The partition function for an arbitrary value of B is given by

$$Z_N(B, J, T) = \int \cdots \int \prod_{i=1}^N d\Omega_i \exp[-\beta H_N(B, J)], \quad (3)$$

where $d\Omega_i = \sin\theta_i d\theta_i d\varphi_i$ is an element of solid angle appropriate to the i th spin, $\beta = 1/(k_B T)$, k_B is Boltzmann's constant, and T is the absolute temperature of the system. Inasmuch as all spins are equivalent, the magnetic moment per spin induced by the magnetic field is given by $\langle m_z \rangle = \langle M_z \rangle / N$, where

$$\langle M_z \rangle = \mu N \langle S_{iz} \rangle = \frac{1}{\beta} \frac{\partial}{\partial B} \ln Z_N(B, J, T). \quad (4)$$

The susceptibility per spin, $\chi_B(T) = (\partial / \partial B) \langle m_z \rangle$, may be obtained using Eq. (4) but it is also provided by the fluctuation relation in the form

$$\chi_B(T) = \mu^2 \beta \sum_{i=1}^N (\langle S_{iz} S_{iz} \rangle - \langle S_{iz} \rangle^2). \quad (5)$$

In the zero-field limit we have $\langle S_{iz} S_{jz} \rangle = (1/3) \langle \vec{S}_i \cdot \vec{S}_j \rangle$ and $\langle S_{iz} \rangle = 0$, so the zero-field susceptibility per spin, $\chi_0(T)$, may be written as

$$\chi_0(T) = \frac{1}{3} \mu^2 \beta \tilde{\chi}(T), \quad (6)$$

in terms of a reduced susceptibility, $\tilde{\chi}(T)$, given by

$$\tilde{\chi}(T) = 1 + \sum_{j=2}^N \langle \vec{S}_1 \cdot \vec{S}_j \rangle. \quad (7)$$

In the high-temperature limit all of the correlation functions $\langle \vec{S}_1 \cdot \vec{S}_{j \geq 2} \rangle$ vanish and as expected, Eq. (6) reduces to Curie's law.

B. Equilateral triangle

1. Partition function

In this subsection we first derive a formula for the partition function, in the form of a one-dimensional integral, for the equilateral triangle of spins. We then proceed to derive analytic expressions for the magnetic moment per spin and the n-n spin-correlation function as functions of T and B , as well as the zero-field susceptibility.

We start by showing that with the introduction of the total spin vector, $\vec{S} = \vec{S}_1 + \vec{S}_2 + \vec{S}_3$ the calculation of the partition function $Z_3(B, J, T)$ can readily be achieved. The success of our method will hinge on the fact that the Hamiltonian $H_3(B, J)$ may be rewritten solely in terms of \vec{S} , as

$$H_3(B, J) = \frac{J}{2} (S^2 - 3) - \mu \vec{B} \cdot \vec{S}. \quad (8)$$

As it stands the integral in Eq. (3) for $N=3$ is six-dimensional. We note that the value of this integral is left unchanged if we multiply the integrand by the three-dimensional Dirac δ function,

$$\delta^{(3)}(\vec{S}-\vec{S}_1-\vec{S}_2-\vec{S}_3)=\int\frac{d^3k}{(2\pi)^3}\exp[i\vec{k}\cdot(\vec{S}-\vec{S}_1-\vec{S}_2-\vec{S}_3)], \quad (9)$$

and then integrate over \vec{S} . Although we are now faced with a twelve-dimensional integral the subsequent calculations are actually very straightforward. In particular, we exploit the dependence of $H_3(B,J)$ on \vec{S} , rather than the individual unit vectors \vec{S}_i ; the latter appear only in the argument of the exponential of Eq. (9). The integrations over each of the three pairs of angles θ_i, φ_i ($i=1,2,3$) are now trivially performed. The remaining, ostensibly six-dimensional integral depends only on \vec{S} and \vec{k} , although in actual fact it is immediately reducible to a one-dimensional integral of the form

$$Z_3(a,b)=(4\pi)^3\exp\left(\frac{3}{2}a\right)K(a,b), \quad (10)$$

where

$$K(a,b)=\int_0^3dSD_3(S)\exp\left(-\frac{a}{2}S^2\right)\frac{\sinh(bS)}{bS}, \quad (11)$$

where we introduce the dimensionless quantities $a=\beta J$, $b=\mu\beta B$, and $D_3(S)$ denotes the integral

$$D_3(S)=4\pi S^2\int\frac{d^3k}{(2\pi)^3}\exp(i\vec{k}\cdot\vec{S})\left(\frac{\sin k}{k}\right)^3. \quad (12)$$

Now one can readily evaluate the latter integral with the result

$$D_3(S)=\begin{cases} S^2/2, & 0\leq S\leq 1 \\ S(3-S)/4, & 1\leq S\leq 3 \\ 0, & S\geq 3. \end{cases} \quad (13)$$

Note that $D_3(S)$ is continuous at the merger points $S=1,3$ but its first derivative is discontinuous at these points. As expected for the case of three unit spins, contributions to $Z_3(a,b)$ can only arise from values of S in the interval $(0,3)$; hence $D_3(S)$ must necessarily vanish for $S>3$, and the upper limit in Eq. (11) reflects this. One can evaluate $K(a,b)$ in closed form and the final result for $Z_3(a,b)$ is

$$\begin{aligned} \frac{Z_3(a,b)}{(4\pi)^3} &= \frac{1}{4ab}[\exp(-3a)\sinh(3b)-3\exp(a)\sinh(b)] \\ &+ \sqrt{\frac{\pi}{2a}}\frac{\exp[3a/2+b^2/(2a)]}{8ab} \\ &\times \left[3(a+b)\operatorname{erf}\left(\frac{a+b}{\sqrt{2a}}\right)-3(a-b)\operatorname{erf}\left(\frac{a-b}{\sqrt{2a}}\right) \right. \\ &\left. - (3a+b)\operatorname{erf}\left(\frac{3a+b}{\sqrt{2a}}\right)+(3a-b)\operatorname{erf}\left(\frac{3a-b}{\sqrt{2a}}\right) \right], \end{aligned} \quad (14)$$

where $\operatorname{erf}(z)$ denotes the familiar error function (see, for example, Chap. 7 of Ref. 16), which is defined for any value of the complex variable z . The properties of this function which are useful in the present setting, including its connection with the confluent hypergeometric function, and its asymptotic properties for large real and large imaginary argument, are listed in the Appendix. In writing Eq. (14) we have reached our goal of obtaining $Z_3(a,b)$ in a form valid for either AFM or FM exchange interactions.

2. $T=0$ K

Before proceeding to extract physical results from Eq. (10), we consider the limiting case of $T=0$ K. For cases of AFM exchange the energy expression, Eq. (8), is minimized for given B when \vec{S} is directed parallel to \vec{B} and when its magnitude is given by $S=\mu B/J$. The linear growth of S with increasing B applies for the regime $B<B_c$, where $B_c\equiv 3J/\mu$. By contrast, we have $S=3$ for $B>B_c$. For the regime $B<B_c$ the explicit expression for the minimum energy $E_0(B,J)$ is given by $E_0(B,J)=-(3/2)J-(\mu B)^2/(2J)$, and thus the equilibrium spin-correlation function is given by

$$\langle\vec{S}_1\cdot\vec{S}_2\rangle=\frac{1}{3}\frac{\partial E_0(B,J)}{\partial J}=-\frac{1}{2}+\frac{1}{6}\left(\frac{\mu B}{J}\right)^2 \quad (T=0\text{ K}, B<B_c). \quad (15)$$

Note that, in the zero-field limit each spin can be pictured as being oriented with an angle of 120° [$=\cos^{-1}(-1/2)$] with respect to each of its two neighbors. This frustrated order is modified as the field is applied, with the spin-correlation function increasing quadratically with B until, when $B\geq B_c$, it reaches the value unity (spins are collinear). For FM exchange and for $T=0$ K the spins are collinear for any value of B .

3. General T, B

Turning now to nonzero temperatures, we first discuss the field dependence of the total magnetic moment of the system for fixed temperature. This quantity is given by the standard thermodynamic relation

$$\langle M_z\rangle=\mu\frac{\partial}{\partial b}\ln Z_3(a,b). \quad (16)$$

Using Eq. (10) and performing the differentiation prescribed in Eq. (16), one finds

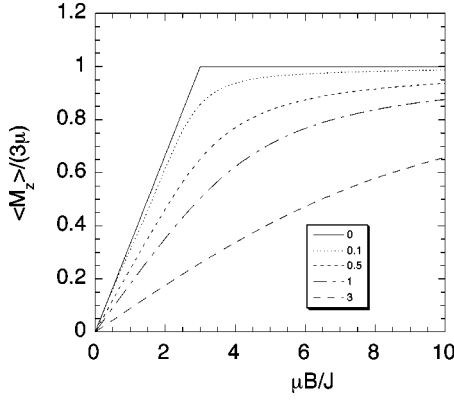


FIG. 1. Field-induced total magnetic moment per spin for a ring of $N=3$ classical Heisenberg spins with AFM exchange for values of $k_B T/J$ listed in the legend. The low-field susceptibility remains finite in the low-temperature limit as a result of frustrated magnetic ordering.

$$\frac{\langle M_z \rangle}{\mu} = \frac{1}{b} \left(\frac{K_1(a,b)}{K(a,b)} - 1 \right), \quad (17)$$

where

$$K_1(a,b) = \int_0^3 dS D_3(S) \exp\left(-\frac{a}{2} S^2\right) \cosh(bS), \quad (18)$$

and $K(a,b)$ has already been defined in Eq. (11). For weak fields the quantity in parenthesis in Eq. (17) is of second order in b and thus $\langle M_z \rangle / \mu$ is of first order, as expected. For arbitrary fields it is straightforward to evaluate the integrals in Eq. (18) and Eq. (11) using standard numerical integration methods. In Fig. 1 we display our results for $\langle M_z \rangle / (3\mu)$, the magnetic moment per spin in units of μ , as a function of $\mu B/J$ for several values of a , for AFM coupling. The results derived in the previous subsection for $T=0$ K are also included.

The corresponding results for FM coupling are given in Fig. 2. One observes that the major difference between the two figures is that for AFM exchange the zero-field susceptibility $\chi_0(T)$ remains finite in the low-temperature limit, whereas it diverges for FM exchange. This is a direct consequence of the fact that in the case of AFM exchange the

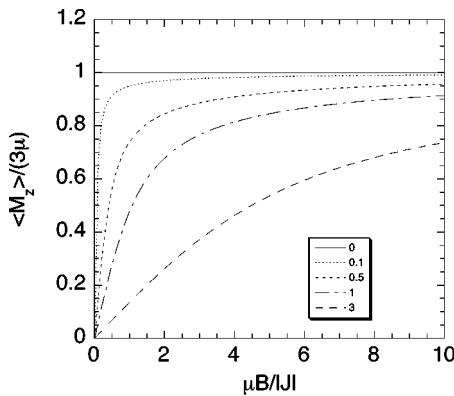


FIG. 2. Field-induced total magnetic moment per spin for a ring of $N=3$ classical Heisenberg spins with FM exchange for values of $k_B T/J$ listed in the legend. The low-field susceptibility diverges in the low-temperature limit as expected for ferromagnetic ordering.

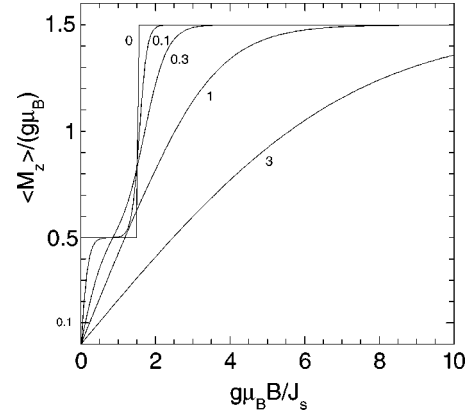


FIG. 3. Field-induced total magnetic moment of a ring of $N=3$ spin $1/2$ particles with AFM exchange. The curves are labeled by the numerical value of the dimensionless parameter $k_B T/J_S$, where J_S is the exchange interaction between the quantum spins. The rapid change in $\langle M_z \rangle$ versus B at low temperatures is due to the ground-state level crossing that occurs when $B=B_c$, where $g\mu_B B_c/J_S=3/2$; the ground state has total spin quantum number $S=1/2$ ($3/2$) for $B<(>)B_c$.

reduced zero-field susceptibility $\tilde{\chi}(T)$ vanishes in the limiting case of low- T and low- B values because, as seen from Eq. (15), the spin-correlation function approaches the value $-1/2$. That is, the low-temperature finite limit of $\chi_0(T)$ is a direct manifestation of the AFM order. A more detailed discussion of $\chi_0(T)$ is provided in the following subsection.

It is of interest to compare Fig. 1 with the easily derived corresponding figure appropriate to the $N=3$ spin- $1/2$ Heisenberg model of ion spins with AFM exchange interaction ($J_S > 0$). Shown in Fig. 3 is the total equilibrium magnetic moment in units of $g\mu_B$ for the latter model versus $g\mu_B B/J_S$ for several choices of $k_B T/J_S$. The dramatic feature in the latter figure is the very rapid change in magnetic moment that occurs for very small changes of B for fixed, low temperatures. Those rapid changes are quantum in origin, being a direct expression of the ground-state–first-excited state energy level crossings as the field is increased.

In particular, the changes in $\langle \hat{M}_z \rangle$, at sufficiently low temperature are especially striking in the immediate vicinity of the field value $g\mu_B B/J_S=3/2$ for which the ground state (total spin $S=1/2$, $M_S=1/2$) and the first excited state (total spin $S=3/2$, $M_S=3/2$) become degenerate, and there is negligible occupancy of all other states. For relatively small values of quantum spin S , exact numerical results can be obtained using standard diagonalization methods. In Fig. 4 we show the magnetic moment per spin in units of $\mu = g\mu_B \sqrt{S(S+1)}$ versus $\mu B/J$, where $J=S(S+1)J_S$, and for $k_B T/J=0.3$ for the $N=3$ quantum Heisenberg rings. The solid curves shown are for spins $S=1/2, 1, 3/2, 2, 5/2, 7/2$, and $11/2$. The dashed curve is the corresponding result for the classical Heisenberg model. For increasing values of S the curves rapidly converge to the classical curve, although one notes that for lower values of temperature we need higher values of S in order to achieve a good convergence to the classical result. In the classical limit, i.e., individual spins S with $S \rightarrow \infty$, the Heisenberg Hamiltonian can be visualized in terms of a continuous distribution of eigenvalues for any

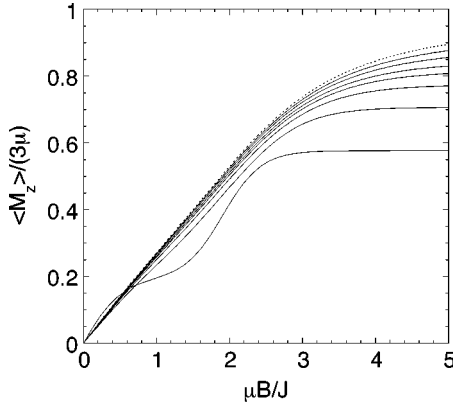


FIG. 4. Field-induced magnetic moment per spin in units of $\mu = g\mu_B\sqrt{S(S+1)}$ as a function of $\mu B/J$ for a quantum ring of $N = 3$ spin- S particles with AFM exchange interaction ($J_S > 0$) and for $k_B T/J = 0.3$, where $J = S(S+1)J_S$. The curves shown are for $S = 1/2$ (lowest curve), 1, 3/2, 2, 5/2, 7/2, 11/2, and for the classical Heisenberg model (dashed curve).

value of the magnetic field, and thus there is an absence of rapid changes in the magnetic moment of the system that occur for $S = 1/2$.

Returning to the $N = 3$ classical Heisenberg ring, the n - n spin-correlation function can be obtained using the formula

$$\langle \vec{S}_1 \cdot \vec{S}_2 \rangle = -\frac{1}{N} \frac{\partial}{\partial a} \ln Z_N(a, b), \quad (19)$$

which for $N = 3$ leads to the result

$$\langle \vec{S}_1 \cdot \vec{S}_2 \rangle = -\frac{1}{2} + \frac{1}{6} \frac{K_2(a, b)}{K(a, b)}. \quad (20)$$

The function $K_2(a, b)$ is defined by

$$K_2(a, b) = \int_0^3 dS D_3(S) S^2 \exp\left(-\frac{a}{2} S^2\right) \frac{\sinh(bS)}{bS}, \quad (21)$$

and is easily evaluated by numerical integration methods. In Fig. 5 we provide our results for the spin-correlation function as a function of $\mu B/J$ for several choices of $k_B T/J$ for AFM exchange. The details of the curve corresponding to the $T = 0$ case have been discussed in the previous subsection, and in particular we recall that for $B = 0$ the three spins can be pictured as lying in a common plane with an angle of 120° between successive spins. For $0 < \mu B/J < 3$ the correlation function is given by Eq. (15), whereas the spins are collinear if $\mu B/J \geq 3$. By contrast, for any nonzero temperature the spins become collinear only asymptotically in the large- B limit. We also note that the value of $\mu B/J$ for which the three spins may be pictured as mutually orthogonal, i.e., when $\langle \vec{S}_1 \cdot \vec{S}_2 \rangle$ vanishes, increases monotonically with increasing temperature.

For the corresponding $N = 3$ spin-1/2 Heisenberg model with AFM exchange, one can readily derive the spin-correlation function, as a function of $g\mu_B B/J_S$, and it is shown in Fig. 6. For this system the common high-field limit of the family of curves is of course given by $+1/4$. Note that for the case $T = 0$ the correlation function is piecewise con-

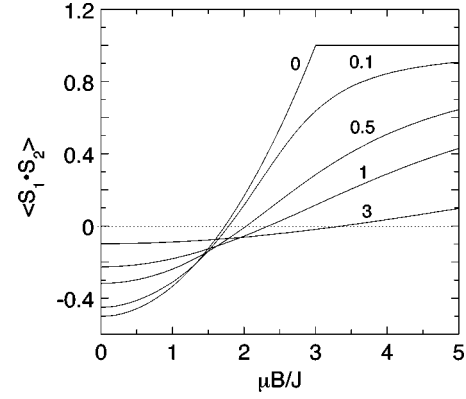


FIG. 5. Nearest-neighbor spin-correlation function for a ring of $N = 3$ classical Heisenberg spins with AFM exchange as a function of magnetic field. The curves are labeled by the numerical value of the dimensionless parameter $k_B T/J$. For low magnetic fields B the frustrated spin ordering persists over a rather wide-temperature interval.

stant, being equal to $-1/4$ when $g\mu_B B/J_S < 3/2$ and equal to $+1/4$ when $g\mu_B B/J_S > 3/2$. This behavior is a direct consequence of the ground-state–first-excited-state energy level crossing, discussed earlier in this subsection, which occurs for $g\mu_B B/J_S = 3/2$.

In Fig. 7 we show the dependence of the spin-correlation function of the classical $N = 3$ Heisenberg ring with AFM exchange on the variable $k_B T/J$ for several values of $\mu B/J$. We have already remarked that $\langle \vec{S}_1 \cdot \vec{S}_2 \rangle = 1$ at $T = 0$ if $\mu B/J \geq 3$. The new features are, first, the diverging slope of the curve corresponding to $\mu B/J = 3$ in the limit $k_B T/J \rightarrow 0$, and second, the merging of the family of curves for sufficiently large values of $k_B T/J$.

In Fig. 8 we display, for this same quantum system, the spin-correlation function versus $k_B T/J_S$ for several values of $g\mu_B B/J_S$. Note the qualitative difference in the low-temperature behavior according to whether $g\mu_B B/J_S$ is less than or exceeds the value $3/2$. For the special case $g\mu_B B/J_S = 3/2$ the correlation function can be shown to be given by

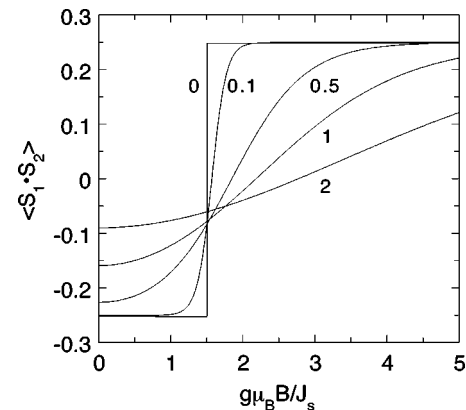


FIG. 6. Nearest-neighbor spin-correlation function for a ring of $N = 3$ Heisenberg spins (individual spins $S = 1/2$) with AFM exchange as a function of magnetic field. The curves are labeled by the numerical value of the dimensionless parameter $k_B T/J_S$.

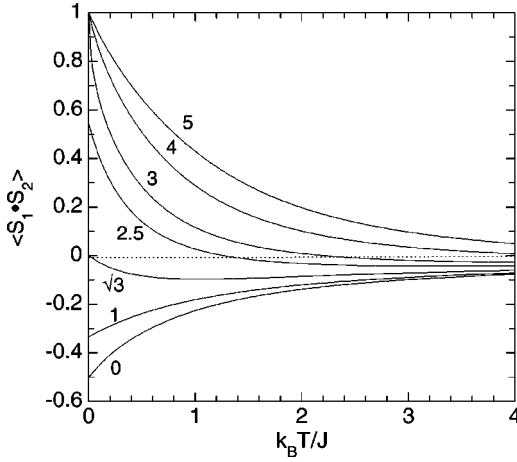


FIG. 7. Nearest-neighbor spin-correlation function for a ring of $N=3$ classical Heisenberg spins with AFM exchange as a function of temperature. The curves are labeled by the numerical value of the dimensionless parameter $\mu B/J$. For low temperatures, as B is increased the frustrated spin ordering gradually gives way to alignment of the spins parallel to the magnetic field.

$$\langle \hat{S}_1 \cdot \hat{S}_2 \rangle = \frac{1}{4} - \frac{1}{3 + \exp(-3\beta J_S)}, \quad (22)$$

and in particular this function approaches the value $-1/12$ in the low-temperature limit. The features shown in Fig. 8 are all readily explained in terms of the ground-state–first-excited state level crossing.

4. $B=0$

In this subsection we show that in the zero-field limit we can obtain results in closed form for the spin-correlation function and $\tilde{\chi}(T)$. We note that in this limit ($b \rightarrow 0$) the factor $\sinh(bS)/(bS)$ in the integrand of Eq. (11) equals unity, and one readily obtains the result

$$Z_3(a, b=0) = (4\pi)^3 \exp\left(\frac{3}{2}a\right) \frac{1}{8a} \sqrt{\frac{2\pi}{a}} \times \left[3 \operatorname{erf}\left(\sqrt{\frac{a}{2}}\right) - \operatorname{erf}\left(3\sqrt{\frac{a}{2}}\right) \right]. \quad (23)$$

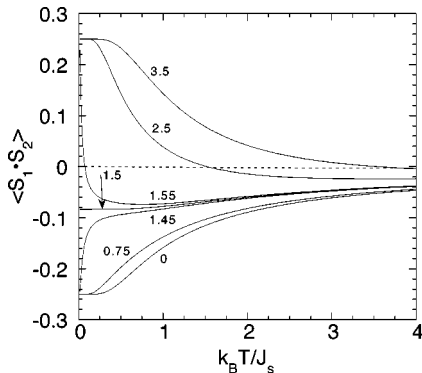


FIG. 8. Nearest-neighbor spin-correlation function for a ring of $N=3$ Heisenberg spins (individual spins $S=1/2$) with AFM exchange as a function of temperature. The curves are labeled by the numerical value of the dimensionless parameter $g\mu_B B/J_S$.

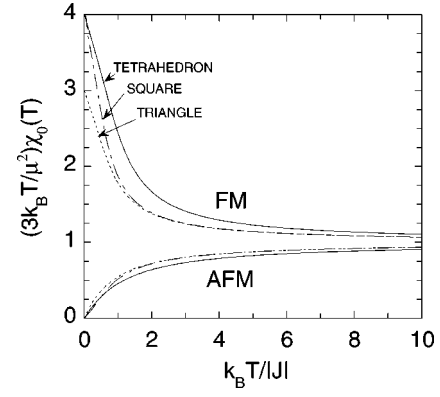


FIG. 9. Reduced zero-field susceptibility per spin, $\tilde{\chi}(T)$ [see Eq. (6)] for equilateral triangle, square, and tetrahedron arrays of classical Heisenberg spins, as a function of the dimensionless parameter $k_B T/|J|$ for FM and AFM exchange interaction.

Of particular physical interest in the zero-field limit is the n-n spin correlation function $\langle \vec{S}_1 \cdot \vec{S}_2 \rangle$ which can be obtained from Eq. (19) and for $N=3$ we find the result

$$\langle \vec{S}_1 \cdot \vec{S}_2 \rangle = -\frac{1}{2} + \frac{1}{2a} - \frac{1}{\sqrt{2\pi a}} \frac{\exp\left(-\frac{a}{2}\right) - \exp\left(-\frac{9}{2}a\right)}{3 \operatorname{erf}\left(\sqrt{\frac{a}{2}}\right) - \operatorname{erf}\left(3\sqrt{\frac{a}{2}}\right)}. \quad (24)$$

This expression can be used for either sign of a , i.e., either AFM or FM coupling. We first consider the case of AFM coupling between n-n spins. In the low-temperature regime ($a \gg 1$), utilizing Eq. (A5) we find

$$\langle \vec{S}_1 \cdot \vec{S}_2 \rangle (T \rightarrow 0) \rightarrow -\frac{1}{2} + \frac{k_B T}{2J}. \quad (25)$$

Besides providing a description of the frustrated spin ordering in the low-temperature limit, Eq. (25) gives quantitative information regarding the leading corrections for low temperatures. In the case of FM coupling, the behavior of $\langle \vec{S}_1 \cdot \vec{S}_2 \rangle$ is very different in the low-temperature regime, as a result of the fact that Eq. (A6) applies. The major conclusion is that, instead of Eq. (25), we obtain the result

$$\langle \vec{S}_1 \cdot \vec{S}_2 \rangle (T \rightarrow 0) \rightarrow 1 - \frac{2k_B T}{3|J|}. \quad (26)$$

In particular, we verify the expected behavior for FM exchange interaction, namely, that in the low-temperature limit the three spins are aligned parallel to each other.

Note that for $N=3$ the relation of Eq. (7) for the reduced zero-field susceptibility per spin may be written as $\tilde{\chi}(T) = 1 + 2\langle \vec{S}_1 \cdot \vec{S}_2 \rangle$. We may then utilize Eq. (24) so as to obtain the explicit functional dependence of $\tilde{\chi}(T)$ on T and the result is displayed in Fig. 9 for both AFM and FM exchange interaction. For very low temperatures one may use Eqs. (24), (25), and (26) to obtain

$$\tilde{\chi}(T \rightarrow 0) \rightarrow \frac{k_B T}{J}, \quad (27)$$

in the AFM case, whereas

$$\tilde{\chi}(T \rightarrow 0) \rightarrow 3 - \frac{4k_B T}{3|J|} \quad (28)$$

in the FM case. The latter formula is a special case of the general result, self-evident from Eq. (7), that $\tilde{\chi}(T \rightarrow 0) \rightarrow N$ for a ring with N spins interacting with n-n FM exchange interaction.

It should be noted that for the corresponding¹⁷ quantum Heisenberg system of three spins-1/2 one finds that for AFM exchange interaction $\tilde{\chi}(T) = (1/4)[3 - 2 \tanh(3\beta J_S/4)]$, and this quantity decreases monotonically from the value 3/4 for $T = \infty$ to the finite nonzero value, 1/4, in the low-temperature limit, contrary to the result of Eq. (27). That is, $\chi_0(T)$ diverges proportionally to $1/T$ for the quantum system with AFM exchange. This behavior at low temperatures is already evident in Fig. 3. A closely related result is that the n-n spin-correlation function for this quantum system when $B = 0$ is given by $\langle \hat{S}_1 \cdot \hat{S}_2 \rangle = -(1/4) \tanh(3\beta J_S/4)$.

C. Tetrahedron

In this subsection we list the major formulas for the tetrahedron system where a single classical spin occupies each vertex. Each spin interacts with its three neighbors via the same isotropic Heisenberg exchange as well as with a uniform B field. Following the method described in Sec. II A we find that

$$Z(a, b) = (4\pi)^4 \exp(2a) \int_0^4 dS D(S) \exp\left(-\frac{a}{2} S^2\right) \frac{\sinh(bS)}{bS}, \quad (29)$$

where $S = |\vec{S}_1 + \vec{S}_2 + \vec{S}_3 + \vec{S}_4|$ and where $D(S)$ is given by

$$D(S) = \begin{cases} \frac{S^2}{16}(8-3S), & 0 \leq S \leq 2 \\ \frac{S}{16}(4-S)^2, & 2 \leq S \leq 4 \\ 0, & S > 4. \end{cases} \quad (30)$$

By contrast to what we found for the three-spin ring, both $D(S)$ and its first derivative are continuous at the merger points $S=2$ and 4. Although in practice it is usually more convenient to work with the expression provided in Eq. (29), one can find an explicit formula for $Z(a, b)$ in closed form. The equilibrium magnetic moment $\langle M_z \rangle / \mu$ versus B and T is readily obtained by numerical integration of the integrals resulting from differentiating the logarithm of Eq. (29) with respect to b . We have also obtained $\langle \vec{S}_1 \cdot \vec{S}_2 \rangle$ as a function of B and T . We do not provide any figures for this system, with the exception of Fig. 9, as they are very similar to those given in Sec. III B for the $N=3$ ring.

In the zero-field limit ($b \rightarrow 0$) limit Eq. (29) is readily evaluated and we obtain

$$Z(a, b=0) = (4\pi)^4 \frac{\exp(2a)}{8a^2} \{ \sqrt{8\pi a} [2 \operatorname{erf}(\sqrt{2a}) - \operatorname{erf}(\sqrt{8a})] + 4 \exp(-2a) - \exp(-8a) - 3 \}. \quad (31)$$

Since the four spins are completely equivalent, the zero-field n-n spin-correlation function $\langle \vec{S}_1 \cdot \vec{S}_2 \rangle$ is easily calculated using the relation $\langle \vec{S}_1 \cdot \vec{S}_2 \rangle = (\langle S^2 \rangle - 4)/12$ and we find that

$$\langle \vec{S}_1 \cdot \vec{S}_2 \rangle = -\frac{1}{3} + \frac{1}{4a} + \frac{1}{12a} \frac{4 \exp(-2a) - \exp(-8a) - 3}{\sqrt{8\pi a} [2 \operatorname{erf}(\sqrt{2a}) - \operatorname{erf}(\sqrt{8a})] + 4 \exp(-2a) - \exp(-8a) - 3}. \quad (32)$$

This expression is valid for either sign of a but its behavior in the zero-temperature limit is very different for the two cases. Concentrating our attention on the AFM case we find that in the zero-temperature limit

$$\langle \vec{S}_1 \cdot \vec{S}_2 \rangle (T \rightarrow 0) \rightarrow -\frac{1}{3} + \frac{k_B T}{4J}. \quad (33)$$

We observe that at $T=0$ the four AFM coupled spins in the tetrahedron can be pictured as oriented in such a way as to give zero total spin and with an angle equal to $\cos^{-1}(-1/3)$ between any pair of spins. The reduced zero-field susceptibility can be computed for any temperature using the relation $\tilde{\chi}(T) = 1 + 3\langle \vec{S}_1 \cdot \vec{S}_2 \rangle$ as well as Eq. (32). We find that in the low-temperature limit $\tilde{\chi}(T \rightarrow 0) \rightarrow 3k_B T/(4J)$ for AFM coupling, while for FM exchange $\tilde{\chi}(T \rightarrow 0) \rightarrow 4$. In

short, the spins exhibit frustration as for the $N=3$ ring and qualitatively in the same manner.

D. Dimer

For the sake of completeness we summarize a few results for the ring of $N=2$ spins (dimers) whose interaction is described by the Hamiltonian $H_2(B, J)$ that is specifically written as

$$H_2(B, J) = J' \vec{S}_1 \cdot \vec{S}_2 - \mu \vec{B} \cdot (\vec{S}_1 + \vec{S}_2), \quad (34)$$

where $J' = 2J$. Again following the method of Sec. II B, we find that the partition function is given by

$$Z_2(a,b) = (4\pi)^2 \exp(2a) \int_0^2 dS D_2(S) \exp(-aS^2) \frac{\sinh(bS)}{bS}, \quad (35)$$

and $D_2(S)$ is given by

$$D_2(S) = \begin{cases} S/2, & 0 < S < 2 \\ S/4, & S = 2 \\ 0, & S > 2. \end{cases} \quad (36)$$

Evaluating Eq. (35) one finds the following relatively compact result

$$Z_2(a,b) = (4\pi)^2 \exp(2a) \frac{\exp\left(\frac{b^2}{4a}\right)}{4b} \sqrt{\frac{\pi}{4a}} \left[\operatorname{erf}\left(\frac{4a-b}{\sqrt{4a}}\right) - \operatorname{erf}\left(\frac{4a+b}{\sqrt{4a}}\right) + 2 \operatorname{erf}\left(\frac{b}{\sqrt{4a}}\right) \right]. \quad (37)$$

The total equilibrium magnetic moment $\langle M_z \rangle$ induced by the magnetic field is given by

$$\frac{\langle M_z \rangle}{\mu} = \frac{b}{2a} - \frac{1}{b} + \frac{1}{\sqrt{\pi a}} \frac{2 \exp\left(-\frac{b^2}{4a}\right) - \exp\left[-\frac{(4a-b)^2}{4a}\right] - \exp\left[-\frac{(4a+b)^2}{4a}\right]}{2 \operatorname{erf}\left(\frac{b}{\sqrt{4a}}\right) + \operatorname{erf}\left[\frac{4a-b}{\sqrt{4a}}\right] - \operatorname{erf}\left[\frac{4a+b}{\sqrt{4a}}\right]}. \quad (38)$$

Since the zero-field partition function is the same for both AFM and FM cases and is given by

$$Z_2(a,b=0) = (4\pi)^2 \frac{\sinh(2a)}{2a}, \quad (39)$$

the zero-field spin correlation function is given by $\langle \vec{S}_1 \cdot \vec{S}_2 \rangle = -L(2a)$, where $L(x) = \coth(x) - 1/x$ is the Langevin function. In the low-temperature regime one finds that

$$\langle \vec{S}_1 \cdot \vec{S}_2 \rangle (T \rightarrow 0) \rightarrow \mp 1$$

for AFM and FM exchange, respectively. The reduced zero-field susceptibility follows directly as $\tilde{\chi}(T) = 1 + \langle \vec{S}_1 \cdot \vec{S}_2 \rangle = 1 - L(2a)$ for both the AFM and FM cases.

III. SQUARE

A. Partition function

Evaluation of the partition function, Eq. (3), by analytical methods constitutes a serious challenge for a square array of spins that interact via n-n exchange. However, we have found that this calculation does become tractable upon introducing the pair of auxiliary variables $\vec{S}_a = \vec{S}_1 + \vec{S}_3$, $\vec{S}_b = \vec{S}_2 + \vec{S}_4$ as well as the total spin vector $\vec{S} = \vec{S}_a + \vec{S}_b$. In terms of these variables the Hamiltonian $H_4(B,J)$ may be written as

$$H_4(B,J) = \frac{J}{2} (S^2 - S_a^2 - S_b^2) - \mu \vec{B} \cdot \vec{S}. \quad (40)$$

Following the same approach as in Sec. II, we introduce each of these three auxiliary vectors by multiplying the integrand of Eq. (3) by an appropriate three-dimensional Dirac δ function and then integrate over that vector. Once again an integral representation akin to Eq. (9) is introduced for each of the δ functions. One readily finds the following formula for the partition function,

$$Z_4(a,b) = (4\pi)^4 \int_0^4 dS D_4(S,a) \exp\left(-\frac{a}{2} S^2\right) \frac{\sinh(bS)}{bS}, \quad (41)$$

where $D_4(S,a)$ is the double integral, given, for $0 \leq S \leq 4$, by

$$D_4(S,a) = \frac{S}{8} \int \int_{R(S)} dS_a dS_b \exp\left[\frac{a}{2} (S_a^2 + S_b^2)\right], \quad (42)$$

where the integration is to be performed over the polygonal region labeled $R(S)$, which is shown in Fig. 10. It is easily shown that this region is the locus of all points that fulfill the pair of inequalities $|\vec{S}_a - \vec{S}_b| < S < S_a + S_b$, for values $0 \leq S_a, S_b \leq 2$. It should be noted that $R(S)$ is a triangular region if $2 \leq S < 4$. The function $D_4(S,a)$ is identically zero for $S \geq 4$. Also note that $D_4(S,a)$ is a function of two independent variables, in contrast to the $N=3$ ring system, where the partition function was expressible [see Eqs. (10)–(12)] in terms of a function $D_3(S)$ of a single variable. We have

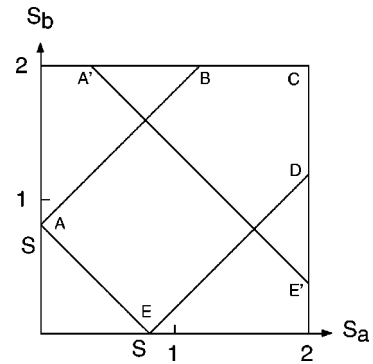


FIG. 10. For the evaluation of the function $D_4(S,a)$ of Eq. (42), the domain of integration $R(S)$ consists of the interior of the polygon $ABCDE$ for the interval $0 \leq S \leq 2$ and the interior of the triangle $A'BCDE'$ for the interval $2 \leq S \leq 4$. For $S \geq 4$, $D_4(S,a)$ is identically zero.

found that it is possible to express the function $D_4(S,a)$ explicitly in terms of confluent hypergeometric functions of assorted variables. The expression is somewhat lengthy and it is available from the authors. One can thus easily obtain numerical values of $D_4(S,a)$ of arbitrarily high accuracy. Numerical evaluation of the one-dimensional integral in Eq. (41) thus reduces to being a very modest and straightforward task. One can generate all thermodynamic quantities of interest by differentiating the logarithm of the integral in Eq. (41) with respect to the variables a and b , thereby producing integrals of a similar form, and thus calculable by numerical methods to any desired level of precision.

B. $T=0$ K

At $T=0$ K and for AFM exchange interaction the energy expression, Eq. (40), is minimized for given B when $S_a=2$, $S_b=2$, and when \vec{S} is directed parallel to \vec{B} and with magnitude $S=\mu B/J$. This linear growth of S with increasing B applies for the regime $B < B_c$, where $B_c \equiv 4J/\mu$. By contrast, we have $S=4$ for $B > B_c$. For the regime $B < B_c$ the explicit form of the minimum energy is given by $E_0(B,J) = -4J - (\mu B)^2/(2J)$, and thus the equilibrium spin-correlation function is given by

$$\langle \vec{S}_1 \cdot \vec{S}_2 \rangle = \frac{1}{4} \frac{\partial E_0(B,J)}{\partial J} = -1 + \frac{1}{8} \left(\frac{\mu B}{J} \right)^2 \quad (T=0 \text{ K}, B < B_c). \quad (43)$$

In particular, in the zero-field limit each spin can be pictured as being antiparallel with respect to each of its two neighbors. As the field is applied, the spin-correlation function increases quadratically with B and reaches the value unity (spins are collinear) as B is increased to or is allowed to exceed the value B_c . As explained, this system does not exhibit frustration for FM exchange and for $T=0$ K the spins are collinear for any value of B .

C. General T , weak magnetic fields

In this subsection we give the formulas for the zero-field susceptibility and the n - n as well as the next-nearest-neighbor (n - n - n) spin-correlation functions for arbitrary temperatures in the weak magnetic field limit. The derivation of these quantities requires the functional form of $Z_4(a,b)$ through second order in the magnetic field. We will not present any specific results for magnetic fields of arbitrary strength because the mathematical analysis becomes quite complex and the results provide little new insight.

Referring back to Eq. (41) and expanding the field-dependent term $\sinh(bS)/(bS)$ to second order in b , one has

$$Z_4(a,b) = Z_4(a,b=0) + b^2 Y_4(a) + O(b^4), \quad (44)$$

where

$$Y_4(a) = \frac{1}{6} (4\pi)^4 \int_0^4 dS S^2 D_4(S,a) \exp\left(-\frac{a}{2} S^2\right). \quad (45)$$

It thus follows that the zero-field susceptibility per spin is given by

$$\chi_0(T) = \frac{1}{2} \mu^2 \beta \frac{Y_4(a)}{Z_4(a,b=0)}. \quad (46)$$

Evaluation of $Z_4(a,b=0)$ is quite straightforward with the result being

$$Z_4(a,b=0) = (4\pi)^4 \frac{F(4a)}{4a^2}, \quad (47)$$

where the function¹⁸ $F(z)$ is defined as

$$F(z) = \int_0^1 du \frac{\cosh(uz) - 1}{u} = F(-z). \quad (48)$$

This function is analytic in the entire finite complex z plane and thus its Taylor expansion in powers of z has an infinite radius of convergence. The Taylor expansion follows immediately upon substituting that of the function $\cosh(uz)$ in Eq. (48) and integrating term by term, with the result being

$$F(z) = \sum_{n=1}^{\infty} \frac{z^{2n}}{(2n)(2n)!}. \quad (49)$$

Also important for the present study are the leading two terms of the asymptotic expansion of $F(z)$ for large real positive or negative values of z , given by

$$F(z) \sim \frac{1}{2} \frac{\exp(|z|)}{|z|} \left[1 + \frac{1}{|z|} + O\left(\frac{1}{|z|^2}\right) \right], \quad (50)$$

as can easily be confirmed by starting from Eq. (48) and integrating several times by parts.

Starting from the above result for $Z_4(a,b=0)$ and using Eq. (19), we find that the zero-field n - n spin-correlation function is given by

$$\langle \vec{S}_1 \cdot \vec{S}_2 \rangle = \frac{1}{2a} \left(1 - \frac{\cosh(4a) - 1}{2F(4a)} \right). \quad (51)$$

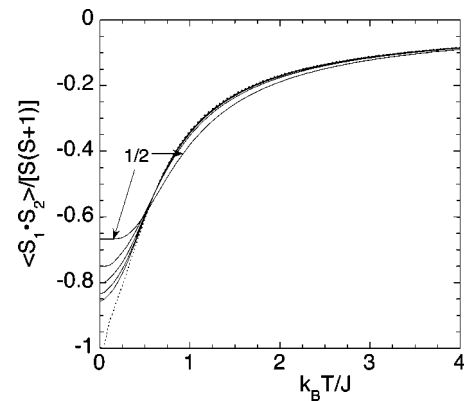


FIG. 11. Normalized nearest-neighbor spin-correlation function for a ring of $N=4$ quantum Heisenberg spins $S=1/2, 1, 3/2, 2, 5/2$ with AFM exchange interaction as a function of $k_B T/J$ where $J = S(S+1)J_S$ for zero magnetic field. The dashed curve is the result for the classical Heisenberg model. At zero temperature the normalized spin-correlation function $\langle \hat{S}_1 \cdot \hat{S}_2 \rangle / [S(S+1)]$ is given by $-(2S+1)/(2S+2)$.

Note that $\langle \vec{S}_1 \cdot \vec{S}_2 \rangle$ is an odd function of a , so that for the same value of $|J|$ and for the same temperature the value of this quantity for FM exchange has the opposite sign of the corresponding quantity for AFM exchange.

It is of interest to compare this result with the corresponding $N=4$ quantum Heisenberg ring of spin S ions with n-n AFM exchange interaction $J_S > 0$. In Fig. 11 we show the n-n spin correlation function $\langle \vec{S}_1 \cdot \vec{S}_2 \rangle / [S(S+1)]$ as a function of $k_B T / J$, where $J = S(S+1)J_S$ for the quantum spin values $S = 1/2, 1, 3/2, 2$, and $5/2$. Once again we observe the rapid convergence of quantum results to that of the classical Heisenberg model for increasing values of S .

Using Eq. (50) it follows that for very low temperatures ($|a| \gg 1$) we have

$$\langle \vec{S}_1 \cdot \vec{S}_2 \rangle (T \rightarrow 0) \rightarrow \pm \left(1 - \frac{3}{4} \frac{k_B T}{|J|} \right) \quad (52)$$

to leading order in the small quantity $k_B T / |J|$, where the upper (lower) sign applies to the case of FM (AFM) exchange. Finally, using Eq. (49) the leading behavior of $\langle \vec{S}_1 \cdot \vec{S}_2 \rangle$ for the high-temperature regime is given by

$$\langle \vec{S}_1 \cdot \vec{S}_2 \rangle (T \rightarrow \infty) \rightarrow -\frac{2}{3} \frac{J}{k_B T}. \quad (53)$$

The evaluation of the function $Y_4(a)$ is very tedious. We find as our final result

$$Y_4(a) = \frac{1}{3} (4\pi)^4 G(4a), \quad (54)$$

where the new function $G(x)$ is given by

$$G(x) = \frac{8}{x^2} \left[\frac{4}{x} F(x) + \frac{2}{x} [1 - \exp(-x)] - \frac{2}{x^2} [\cosh(x) - 1] - 1 \right]. \quad (55)$$

Substitution of Eqs. (54) and (55) into Eq. (46) provides $\chi_0(T)$. The result that one obtains in the high-temperature limit reduces to Curie's law. For very low temperatures the limiting form of the reduced susceptibility $\tilde{\chi}(T) = (3/2)Y_4(a)/Z_4(a, b=0)$ is given by $\tilde{\chi}(T \rightarrow 0) \rightarrow k_B T / (2J)$ for AFM exchange interactions, and by $\tilde{\chi}(T \rightarrow 0) \rightarrow 4 - 5k_B T / (2|J|)$ for FM exchange. The reduced susceptibility is shown in Fig. 9 for rings with $N=3, 4$ and for the tetrahedron. We have already commented that in the case of FM exchange the low-temperature limit should equal the number of spins of the given system. What is perhaps surprising is that as the temperature is increased, already for $k_B T / |J| \approx 1$ the results for the two ring systems have merged. For this temperature and above, the correlations between spins reflect the fact that each spin of the ring interacts with only two nearest-neighbors. For the tetrahedron array each spin interacts with three nearest-neighbors and this is reflected in the larger value of $\tilde{\chi}(T)$. Finally, we note that the n-n-n spin-correlation function $\langle \vec{S}_1 \cdot \vec{S}_3 \rangle$ follows directly

from [see Eq. (7)] the relation $\tilde{\chi}(T) = 1 + 2\langle \vec{S}_1 \cdot \vec{S}_2 \rangle + \langle \vec{S}_1 \cdot \vec{S}_3 \rangle$ along with Eqs. (46) and (51).

IV. SUMMARY

In this paper we have studied in detail the properties of several classical Heisenberg magnetic systems consisting of small numbers of spins coupled by n-n isotropic exchange interaction and that interact with a uniform external magnetic field. By using a method that introduces auxiliary spin variables into the defining expression for the partition function, we obtained the exact analytical formulas for the magnetic moment induced by the external magnetic field for arbitrary temperature (i.e., the complete magnetic equation of state), as well as the field and temperature dependence of the n-n spin-correlation function. The systems considered were small arrays of interacting spins, and specifically dimer, equilateral triangle, square, and regular tetrahedron geometries. For all of these systems we succeeded in expressing the partition function, the total magnetic moment, and the spin-correlation function as one-dimensional integrals, a representation that is particularly convenient for the purpose of extracting highly accurate numerical values, figures, etc. The special cases of the equilateral triangle and the regular tetrahedron exhibit magnetic frustration for AFM exchange interaction, and we were able to obtain a complete description of the evolution of the frustration as a function of temperature and field. In the special case of the equilateral triangle geometry, we gave detailed comparisons between our results for classical spins and the corresponding quantum system of individual spins $S = 1/2, 1, 3/2, \dots$. The reader can correctly anticipate that as the individual spin quantum number S increases, the rapid changes at low temperatures of magnetic moment versus applied magnetic field rapidly wash out. The rapid changes that occur for the case of $S = 1/2$ are a direct consequence of ground-state level crossings. For increasing S the eigenvalue spectrum proliferates, becoming continuous in the large S limit, and the magnetic moment is a slowly varying function of applied field.

Despite the smallness of the systems we have considered, this study is timely for, as discussed in the Introduction, there is considerable experimental activity at present devoted to the synthesis and physical analysis of large organic molecules in which are embedded a very small number of paramagnetic ions, for dimers and arrays with the geometries of an equilateral triangle, square, and regular tetrahedron. A very common choice^{5,10} of paramagnetic ion is Fe^{3+} which has spin $S = 5/2$ and for which the present results are directly applicable, except for sufficiently low temperatures. There are even indications¹⁹ that a classical Heisenberg model provides a very satisfactory description of a ring of eight Cr^{3+} ions, (ion spin $3/2$), again except at low temperatures. To compare theory with the results of experimental NMR and neutron-scattering studies of these molecular magnets it will be necessary to utilize expressions for the general space-time two-spin-correlation functions. These theoretical expressions have been derived and will be presented elsewhere.¹⁵ In fact, the present results provide some of the vital ingredients for those derivations.

What are the prospects for succeeding in generalizing the present work to larger arrays of interacting Heisenberg spins,

including more complicated geometries? The trick of introducing two new auxiliary spin vectors, as we did in Sec. III for the ring of four spins, does not seem to be open to generalization for rings with five or more spins and n-n interactions. However, for specialized geometries and interactions, generalizations of the present methods are indeed possible. One example is that of a tetrahedron where three of the four spins interact with each other with one common value of the coupling constant that in turn differs from that coupling the three spins to the fourth spin. The complex known as Fe4 is well described¹⁰ by such a model. For AFM exchange it turns out that the magnetic frustration of this system is a very intricate function of temperature, magnetic field, and the ratio of the two coupling constants.²⁰ A second example is that of an arbitrary number N of spins that interact with all others via a common isotropic exchange constant. This is the isotropic classical Heisenberg analogue of the well-known Kittel-Shore model,²¹ which involves interacting Ising spins. A third example is that of an array of six spins positioned at the vertices of a regular octahedron. It turns out²² that this system also exhibits very interesting frustration effects. Whereas in the past these and other small systems might have been considered as appropriate “recreational” projects for mathematical physicists, because of the dramatic recent advances in synthesis chemistry these models are currently of considerable experimental importance.

ACKNOWLEDGMENTS

Ames Laboratory is operated for the U.S. Department of Energy by Iowa State University under Contract No. W-7405-Eng-82. M.L. thanks P. C. Canfield and Z. H. Jang of Ames Laboratory for useful discussions. M.A. thanks B. Harmon and V. Antropov for their kind hospitality during his visit at Ames Laboratory.

APPENDIX A

For convenience we list here several formulas for the error function $\text{erf}(z)$ that are germane to the present work. For

any complex variable z this function is defined by

$$\text{erf}(z) = \frac{2}{\sqrt{\pi}} \int_0^z dt e^{-t^2}. \quad (\text{A1})$$

Note that $\text{erf}(-z) = -\text{erf}(z)$ and its Taylor expansion,

$$\text{erf}(z) = \frac{2}{\sqrt{\pi}} \sum_{n=0}^{\infty} \frac{(-1)^n z^{2n+1}}{n!(2n+1)}, \quad (\text{A2})$$

converges for all finite z . The relation

$$\text{erf}(z) = \frac{2z}{\sqrt{\pi}} M\left(\frac{1}{2}, \frac{3}{2}, -z^2\right) = \frac{2z}{\sqrt{\pi}} \exp(-z^2) M\left(1, \frac{3}{2}, z^2\right), \quad (\text{A3})$$

proves to be very helpful, where

$$M(a, b, z) = \sum_{n=0}^{\infty} \frac{(a)_n z^n}{(b)_n n!}, \quad (\text{A4})$$

denotes the confluent hypergeometric function (see Chap. 13 of Ref. 16), $(a)_0 = 1$, and $(a)_n = a(a+1)(a+2)\cdots(a+n-1)$ for $n \geq 1$. With the aid of Eq. (A3), one can establish the following two asymptotic formulas that are of importance in the main text for investigating the low-temperature properties of the spin systems. If x denotes a real positive variable, we have for the $x \gg 1$ regime

$$\text{erf}(x) \sim 1 - \frac{1}{\sqrt{\pi}} \frac{\exp(-x^2)}{x} \left[1 - \frac{1}{2x^2} + O\left(\frac{1}{x^4}\right) \right], \quad (\text{A5})$$

and

$$\text{erf}(ix) \sim \frac{i}{\sqrt{\pi}} \frac{\exp(x^2)}{x} \left[1 + \frac{1}{2x^2} + O\left(\frac{1}{x^4}\right) \right], \quad (\text{A6})$$

where $i = \sqrt{-1}$.

¹D. Gatteschi, A. Caneschi, L. Pardi, and R. Sessoli, *Science* **265**, 1054 (1994); D. Gatteschi, *Adv. Mater.* **6**, 634 (1994); *Magnetic Molecular Materials*, Vol. 198 of *NATO Advanced Studies Institute, Series E: Applied Sciences*, edited by D. Gatteschi, O. Kahn, J. S. Miller, and F. Palacio (Kluwer Academic, Norwell, MA, 1991).
²J. R. Friedman, M. P. Sarachik, J. Tejada, and R. Ziolo, *Phys. Rev. Lett.* **76**, 3830 (1996); L. Thomas, F. Lonti, R. Ballou, D. Gatteschi, R. Sessoli, and B. Barbara, *Nature (London)* **383**, 145 (1996).
³*Nanomagnetism*, Vol. 247 of *NATO Advanced Studies Institute, Series E: Applied Sciences*, edited by A. Hernando (Kluwer Academic, Norwell, MA, 1993).
⁴R. J. Bushby and J. L. Paillaud, in *An Introduction to Molecular Electronics*, edited by M. C. Petty, M. R. Bryce, and D. Bloor (Oxford University Press, New York, 1995), pp. 72–91.
⁵Y. Furukawa, A. Iwai, K. I. Kumagai, and A. Yakubovsky, *J. Phys. Soc. Jpn.* **65**, 2393 (1996).

⁶A. Lascialfari, F. Tabak, G. L. Abbati, F. Borsa, M. Corti, and D. Gatteschi, *J. Appl. Phys.* **85**, 4539 (1999).
⁷A. Müller, J. Meyer, H. Bögge, A. Stammler, and A. Botar, *Chem.-Eur. J.* **4**, 1388 (1998).
⁸D. M. Barnhart, D. L. Clark, J. C. Gordon, J. C. Huffman, J. G. Watkin, and B. D. Zwick, *J. Am. Chem. Soc.* **115**, 8461 (1993).
⁹A. Bino, D. C. Johnston, D. P. Goshorn, T. R. Halbert, and E. I. Stiefel, *Science* **241**, 1479 (1988).
¹⁰A. L. Barra, A. Caneschi, A. Cornia, F. Fabrizi de Biani, D. Gatteschi, C. Sangregorio, R. Sessoli, and R. Sorace (unpublished).
¹¹J. S. Gardner, S. R. Dunsiger, B. D. Gaulin, M. J. P. Gingras, J. E. Greedan, R. F. Kiefl, M. D. Lumsden, W. A. MacFarlane, N. P. Raju, J. E. Sonier, I. Swinson, and Z. Tun, *Phys. Rev. Lett.* **82**, 1012 (1999).
¹²M. E. Fisher, *Am. J. Phys.* **32**, 343 (1964).
¹³G. S. Joyce, *Phys. Rev.* **155**, 478 (1967).
¹⁴A numerical method for calculating equilibrium quantities such as

the partition function and equal-time spin-correlation functions has been given by M. Blume, P. Heller, and N. A. Lurie, Phys. Rev. B **11**, 4483 (1975).

¹⁵M. Luban, T. Bandos, and O. Ciftja (unpublished).

¹⁶M. Abramowitz and I. A. Stegun, *Handbook of Mathematical Functions* (Dover, New York, 1965).

¹⁷The zero-field susceptibility per spin for this quantum system is related to a reduced zero-field susceptibility $\tilde{\chi}(T)$ corresponding to Eq. (6), except that $g\mu_B$ replaces μ . However, instead of Eq. (7) we have $\tilde{\chi}(T) = \langle \hat{S}_1 \cdot \hat{S}_1 \rangle + 2\langle \hat{S}_1 \cdot \hat{S}_2 \rangle = 3/4 - \tanh(3\beta J_S/4)/2$,

where J_S is the exchange interaction between quantum spins.

¹⁸It is possible to express the function $F(z)$ in terms of the exponential integral functions $Ei(z)$ and $E_1(z)$, but such an expression is both lengthy and awkward given the fact that each of these functions has a branch point at the origin of the z plane, whereas $F(z)$ is an entire function.

¹⁹A. Bino, D. C. Johnston, M. Luban, and L. Miller (unpublished).

²⁰O. Ciftja and M. Luban, (unpublished).

²¹C. Kittel and H. Shore, Phys. Rev. **138**, A1165 (1965).

²²T. Bandos and M. Luban (unpublished).